

Monte Carlo lattice dynamics studies of binary adsorption in silicalite

L.F. Gladden^{a,*}, M. Hargreaves^a, P. Alexander^b

^aDepartment of Chemical Engineering, University of Cambridge, Pembroke Street, Cambridge, CB2 3RA, UK

^bDepartment of Physics, Cavendish Laboratory, University of Cambridge, Madingley Road, Cambridge, CB3 0HE, UK

Abstract

A highly flexible and efficient Monte Carlo lattice dynamics (MCLD) code has been developed which takes as input data characterising the microdynamics of the adsorbate molecule within the zeolite framework. Molecular dynamics (MD) and grand canonical Monte Carlo (GCMC) simulations are used to determine a physically realistic distribution of adsorption sites within the zeolite and their relative energies of interaction with the adsorbate of interest, these sites are then identified with the lattice sites used in the MCLD simulation. In this paper the method is applied to ethane and ethene adsorbed in silicalite. Variable temperature NMR relaxometry experiments are performed to provide and constrain the input data for the MCLD simulations. Excellent agreement between simulated and measured single- and binary-component adsorption isotherms is obtained and the results are interpreted in terms of the relative rate of site desorption of the two species within the zeolite framework. © 1999 Elsevier Science S.A. All rights reserved.

Keywords: Monte Carlo lattice dynamics; Molecular dynamics; Grand canonical Monte Carlo

1. Introduction

The use of micro-porous materials such as zeolites in catalysis and separations processes is widespread in the petroleum and chemical industries [1]. Central to the use of these materials is a proper understanding of the characteristics of single- and multi-component transport and adsorption processes occurring within the appropriate pore structure. Two main types of numerical simulation methods are used in the study of transport and adsorption in zeolites: Molecular dynamics (MD) and Monte Carlo lattice dynamics simulations (MCLD). In the MD approach [2–5] molecules move within a force field, representing the material and inter-molecular interactions, according to Newton's laws of motion. MCLD studies model the zeolite/adsorbate system as a grid of adsorption sites through which the molecule diffuses via site-to-site jumps [5–7]. The MD method is closer to reality than the MCLD approach and can in principle be used to determine not only information about diffusivities, but also the nature and type of adsorption sites and detailed information on the energetics of adsorbed species. However, MD simulations are computationally very expensive and the number of molecules that can be followed in the simulation is therefore limited. The MCLD approach

on the other hand simplifies the physical model of the detailed interaction and provides a means of simulating sufficiently large systems for correlated and dynamical effects to be determined. Recently van Tassel et al. [5] and Gladden et al. [8] have shown that MCLD simulations can be used as a valuable alternative to MD simulations provided the grid over which the MCLD simulation occurs is a realistic representation of the actual adsorption sites and their connectivity within the zeolite of interest. The importance of reflecting the true connectivity of the zeolite structure in predictions of adsorbate transport within zeolites has also recently been demonstrated by Coppens et al. [9], while Keffer et al. [10] have investigated percolation phenomena in zeolite sorption lattices using MCLD. As input to a MCLD simulation, the rate and activation energy characterising inter-site jump processes of molecules from different types of lattice site are required. In this work ²H NMR relaxation time analysis, in combination with MD simulations, is shown to be an ideal experimental tool to study the dynamics of adsorbed species and can be used to provide direct experimental input to the MCLD simulation. Alternatively, of course, input parameters may be estimated from molecular simulation studies alone. Using the MCLD approach it is possible to simulate both equilibrium (e.g. single- or multi-component adsorption isotherms) and kinetic (e.g. diffusivities) characteristics of the adsorbate–zeolite system of interest.

*Corresponding author. Tel.: +44-1223-334762; fax: +44-1223-334796; e-mail: gladden@cheng.cam.ac.uk

In earlier work we have used ^2H NMR and MCLD simulations to model ethane and ethene single-component adsorption in zeolite NaA [8]. In this paper we discuss in detail a simulation code able to address equilibrium, kinetic and reaction phenomena; the approach is illustrated by predicting the single- and binary-component adsorption isotherms of ethane and ethene in silicalite. This paper is organised as follows. In Section 2 we present a description of the theoretical framework and implementation of the simulation code. In Section 3 the experimental details regarding the acquisition of the ^2H NMR spectra are given. Section 4 presents the ^2H NMR data and the analysis of these in terms of a model of the sorbate motion that allows the NMR results to provide direct input into the simulation code. Section 5 discusses the simulation of the single- and binary-component isotherms taking as input results from the ^2H NMR analysis. The results of the simulations are then used to gain insight into the relative rates of site desorption and adsorption characteristics of the species sorbed within the zeolite.

2. Simulation strategy

2.1. Overview

The simulations are based on a three-dimensional lattice of sites. In general, there are a number of distinct types of site within the lattice which are characterised by different properties (e.g. strength of adsorbate–zeolite interaction) and these lattice sites can be connected so as to represent the true topology and geometry of the adsorbent. Each lattice site is assumed to correspond to an adsorption site in the material and consequently lattice sites usually contain one and only one molecule of any species. A molecule moves through the lattice by jumping from its current site to one of its nearest-neighbour sites, and can jump out of, or into the lattice, to represent desorption and adsorption to/from the gas phase.

The simulation scheme is a Monte Carlo procedure in which the next molecule to be moved within the simulation is chosen on strict probabilistic grounds. In general, let us assume that there are N_E independent events which can occur within the simulation at any time, where each event has a rate μ_n ; these events correspond to the discrete jumps between adsorption sites and into/out of the lattice as discussed above. The next event to occur within the simulation is selected at random, with each possible event being assigned a probability of occurrence proportional to the rate for that event. Having selected an event, for example a jump out of an adsorption site, further decisions relating to this event must be made; for example, the direction of an attempted jump must be determined again based on a probabilistic model. An important element of the simulation strategy is that the event may prove unsuccessful. For example, a molecule may attempt to jump into an occupied

site; these failed events must be handled carefully within the simulation to retain computational efficiency. The implementation of an efficient code is discussed in detail in Section 2.5. For both successful and unsuccessful events the simulation time is incremented according to a Poisson distribution.

In the present paper we shall consider three basic types of process:

1. Jumps between sites within the lattice characterised by a specific rate.
2. Adsorption from the gas phase via jumps into surface sites of the simulation lattice.
3. Desorption to the gas phase via jumps out of the simulation lattice from surface sites of the simulation lattice.

Surface sites are located at the edge of the lattice and are taken to be in contact with an external gas phase. These processes are considered in detail in Section 2.3. The simulation code is quite general and other types of events, such as those representing chemical reaction between adsorbed species can easily be incorporated into the simulation strategy, however these will not be considered further in this paper.

A simple example illustrating the MCLD method is the simulation of adsorption into a regular rectangular lattice. A simple analytical analysis [7] shows that the expected isotherm should have a Langmuir form with the fractional site coverage given by

$$\theta = \frac{\beta}{\Gamma + \beta}, \quad (1)$$

where Γ is the probability per unit time of making a jump from one row to an adjacent row in the zero concentration limit. For a lattice of coordination number κ , $\Gamma=1/\kappa$. This result has been used as a basic test of the simulation code and has been demonstrated to be able to reproduce the expected Langmuir isotherms for lattice coordinations of 3, 4, 5 and 6.

2.2. Simulation lattice

The MCLD lattice is chosen to represent possible adsorption sites, for a given molecular species, within the adsorbent under study. In general the lattice will consist of more sites than would be determined from a purely equilibrium analysis of the adsorption sites within the pore space. Associated with each site is a jump rate, or site-desorption rate, for each molecular species; sites representing the equilibrium adsorption sites of a molecule within a structure will have comparatively low jump rates (long residence times at such sites), whereas other sites, which will be occupied transiently during the simulation will have associated with them a higher jump rate or short residence time. In this way the lattice can be used to properly simulate dynamic and equilibrium processes via the same Monte Carlo approach.

To aid construction of the lattice, MD and grand canonical Monte Carlo (GCMC) simulations provide a powerful technique for the determination of possible adsorption sites and activation energies to molecular jumps from a given site. In this work, the MCLD lattice for C_2 adsorption in silicalite was determined by performing GCMC simulations of ethane and ethene sorbed within the silicalite structure, using the MSI software packages (Catalysis, Discover, Cerius²); full details of this work are discussed elsewhere [11]. In outline, GCMC simulations were performed using the sorption module of the Cerius² software package at various sorbate loadings to determine a spatial probability density, or adsorbate mass distribution, function of where the adsorbate molecules are found within the silicalite framework. Local maxima of this function were identified with adsorption sites. MD simulations were also performed to investigate the dynamics of molecules close to the identified adsorption sites. The MCLD lattice is generated by reproducing the channel structure of silicalite by assigning appropriate connectivity to the lattice sites. The results of the GCMC simulations identify three distinct types of site (type 0, I and II) as shown in Fig. 1, each characterised by different activation energies to molecular desorption. The sites are sufficiently close in space that it is energetically unfavourable to have molecules on adjacent sites, and therefore it is not possible for the 28 distinct sites within the unit cell to be simultaneously occupied; this effect is modelled by introducing a repulsive interaction energy for molecules on adjacent sites as an additional variable, as

discussed in Section 5. Furthermore, the MD simulations identify that the rate of desorption from each of the sites 0, I and II are similar at 300 K, and that the activation energies to desorption from these sites satisfy $E_{II} \approx E_I + 3$ kJ/mol $\approx E_0 + 6$ kJ/mol.

2.3. The Monte Carlo simulation

In this section we consider in detail the Monte Carlo simulation itself. We represent the simulation lattice as a set of sites, s ; for each site an activation energy to desorption for species i , E_{si} , is defined. At least one distinct event can be associated with each occupied site on the lattice and each surface site. For each configuration of lattice and adsorbed molecules the total number of possible events, N_E , can be enumerated and a rate, μ_n , associated with each possible event. The total rate is given by

$$\mu = \sum_n^{N_E} \mu_n, \quad (2)$$

hence the probability of event n occurring is $p_n = \mu_n / \mu$, and the next event to occur within the simulation is selected according to these probabilities. After each event, the simulation time is advanced by an amount δt drawn from a Poisson distribution:

$$P(t) = \mu \exp(-\mu t). \quad (3)$$

Expressions are required for each possible event within the lattice. For molecular jumps between sites within the lattice we consider the process to consist of an activated jump in which the activation energy is determined by molecule-site, E_{si} , and molecule–molecule interactions on first-, $E_{ij}^{(1)}$, and second-nearest-neighbour sites, $E_{ij}^{(2)}$, where i and j are indices identifying each molecular species. For a site connected to κ nearest-neighbours (one or more of which may be external gas) we define the probability of jumping from site s to s' to be $\Gamma(s, s')$, such that

$$\sum_{s'}^{\kappa} \Gamma(s, s') = 1. \quad (4)$$

In general the $\Gamma(s, s')$ factors can represent anisotropic motion through the lattice and may themselves be activated processes or determined by local conditions within the lattice. For example for a zeolite such as NaA in which windows link cages within the zeolite structure, the probability of making a jump between cages through the window is an activated process [8]. The total rate for an event n , that translates the molecule from site s to s' can then be written as

$$\mu_n(i, s, s') = \frac{1}{\tau_i} \Gamma(s, s') = \frac{1}{\tau_{i0}} \exp(-E_{si}/RT) \times \exp \left[- \left(\sum_j n_j^{(1)} E_{ij}^{(1)} + \sum_j n_j^{(2)} E_{ij}^{(2)} \right) / RT \right] \Gamma(s, s'), \quad (5)$$

where $n_j^{(1)}$ and $n_j^{(2)}$ are the number of first- and second-

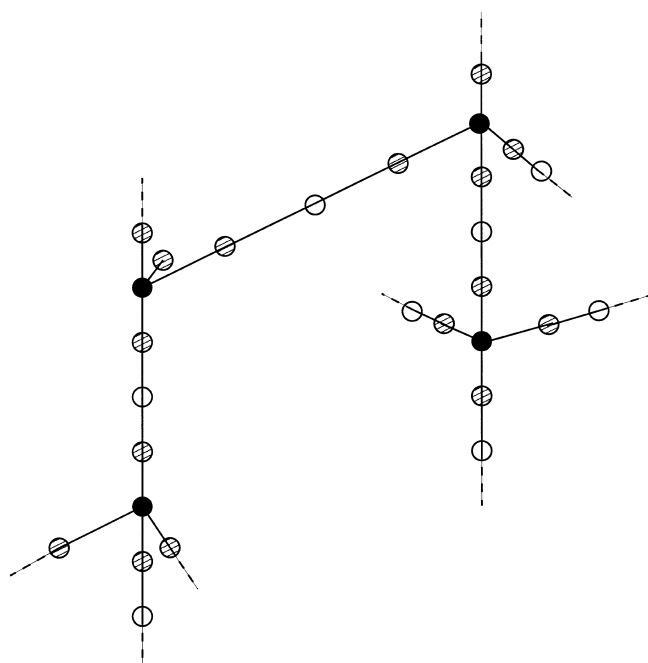


Fig. 1. Simulation lattice for C_2 adsorption in silicalite. Possible jumps are shown by solid lines and jumps to lattice sites not shown are indicated by dashed lines. Three types of site exist associated with different adsorbate-site interaction energies: type 0 (filled circles), type I (hashed circles) and type II (open circles).

nearest-neighbours of species j , respectively, τ_i is the residence time for species i at site s , and τ_{i0} is a pre-exponential factor required when representing the residence time as an activated process. Recently Saravanan et al. [12] have reported a modification to lattice-site jump rates incorporating nearest-neighbour interactions based on a model of overlapping harmonic potentials. Eq. (5) represents a simpler model based on a square-well potential as used by van Tassel et al. [5]; the two approaches agree to first order in energy.

For adsorption processes from the gas phase onto surface sites we consider a kinetic model in which the rate of attempted insertions at site s by species i from the gas phase is given by a temperature dependent factor, β_{si} , such that the rate is simply

$$\mu(i, s) = \beta_{si}. \quad (6)$$

This rate is directly related to the external gas pressure, p , by kinetic theory. The rate of molecular collisions of species i (gas-phase mole fraction y_i) with a surface area, A , of the zeolite is

$$N = \frac{1}{4} \frac{py_i}{k_B T} \bar{c} A, \quad (7)$$

where \bar{c} is the mean velocity of species i in the gas. Not all of these collisions will result in an attempted insertion of the molecule into the interior of the zeolite as many trajectories of the molecule will not reach an adsorption site within the pore space of the zeolite before the molecule interacts with the zeolite and is repelled back into the gas phase. An estimate of the number of such trajectories which fail because of steric effects can be estimated using geometrical arguments [13]. In addition to direct collisions it may be possible for a molecule to make an attempted insertion into the pore space by first adsorbing onto surface sites and then entering the internal pore space of the zeolite by surface diffusion [14]. Both the steric hindrance and surface diffusion effects are difficult to quantify, and are therefore represented by a single factor, α_{si} , that depends on both the molecular species and adsorption site of interest. Using the standard expression for \bar{c} gives the following relationship between pressure and attempted insertion rate:

$$\beta_{si} = \frac{1}{4\alpha_{si}} \frac{py_i}{(2\pi mk_B T)^{1/2}} A. \quad (8)$$

By assuming that only those trajectories from the gas phase which enter directly into a pore in the zeolite lead to adsorption the steric factor may be estimated using the approach of Ford and Glandt [13]. In their approach the probability of a molecule being able to pass through an aperture is determined geometrically by assuming that both the aperture and the molecule are rigid. The steric factor is, however, very uncertain as is the enhancement due to surface diffusion [14] and therefore it is treated in the simulations as a parameter that must be constrained by experiment.

Not all attempted events will succeed. For example, jumps into occupied sites will be forbidden. Conceptually, one can consider the simulation to proceed as follows:

1. For each configuration of the lattice and adsorbed species, enumerate the rates, μ_n , for all possible events and determine the total rate μ .
2. Using these rates, select an event at random with a probability $p_n = \mu_n / \mu$.
3. Increment the simulation time.
4. Check that the chosen event is possible. If it is then update the lattice configuration, if not do nothing.
5. Continue by returning to step (1) and updating the list of possible events (note that a single event may modify many other events).

This procedure is computationally inefficient since considerable computer time is wasted on null-events and on enumerating all possible events at each iteration. Implementation issues relating to this conceptual framework are considered in Section 2.5.

2.4. Simulation of isotherms and self-diffusivity

To simulate single- or multi-component isotherms the lattice is exposed to gas at a fixed composition given by the set of insertion rates β_{si} as given by Eq. (8). The simulation is then allowed to reach a steady state by proceeding with the Monte Carlo simulation allowing for insertions into the lattice and molecular motion within the lattice. Steady-state is determined by monitoring the loading within the simulation lattice; after some number of Monte Carlo iterations the loading for each species reaches a steady-state with a mean fractional site coverage $\langle \theta_i \rangle$ and standard deviation in this parameter, σ_i . Assuming ergodicity, a value for the ensemble averaged loading, $\bar{\theta}_i$, is determined from the temporal average $\langle \theta_i \rangle$ taken over a number of iterations. Typically the simulation runs for a few thousand iterations per adsorbed molecule, requiring approximately 2×10^6 Monte Carlo steps per pressure increment on the isotherm for the simulations considered here.

For the determination of self-diffusivity a typical simulation would involve either letting the simulation reach a steady-state with fixed external conditions, as discussed for the simulation of isotherms, or the lattice can be loaded with a pre-specified loading. In the latter case, the lattice is then “relaxed” for approximately 1000–10 000 iterations per molecule and the Monte Carlo simulation proper is then performed and the development of the system monitored until a steady-state is achieved. During this time periodic boundary conditions are imposed. Each molecule in the simulation lattice is tracked allowing for motion through the periodic boundaries, and the mean square displacement $\langle L^2 \rangle$ is determined as a function of simulation time, t . The self-diffusion coefficient is then calculated from $D = \langle L^2 \rangle / 6t$.

Additionally, the transport diffusivity through the lattice can be determined by exposing two faces of the lattice to external conditions representing different concentrations in the gas phase; periodic boundary conditions are used in the other directions. In this paper we consider binary adsorption of ethane and ethene in silicalite; application of this approach to adsorption and transport phenomena in NaA have been reported elsewhere [8]. In a forthcoming paper we will extend this analysis to predict diffusion behaviour of ethane and ethene in silicalite.

2.5. Implementation considerations

The structure of the simulation code is designed to make it straightforward to undertake different computer experiments with the flexibility to incorporate a range of new events. Furthermore, a number of computational techniques are used to obtain high efficiency without sacrificing flexibility. The simulation code has an embedded scripting language, the Tool Command Language or Tcl [15], which is used to set-up parameters and control the overall execution of the simulation, and an object based structure with the main objects being lattice sites, the lattice, external conditions, molecules and events. This approach provides an extremely flexible tool for MCLD simulations. For example, it is straightforward to implement monitoring of the mean loading of the lattice until steady-state is achieved. In addition Tcl provides a platform-independent I/O library (including support for inter-process communication) that ensures a high degree of portability. The code is structured so that new event types may be added without changing the core application. This is achieved by registering routines that implement the action of each event type, and storing the information in a hash table. The simulation code then uses each of these registered event types via a standard interface. New event types can be added by loading object code into the simulation, again controlled and managed by Tcl.

This flexibility in implementing event types requires an equally flexible approach to finding the next event. Three issues are important: Firstly, to only consider allowed events; secondly, to select an event efficiently; thirdly, to update the list of possible events after the configuration of the lattice/adsorbed molecules has been changed. van Tassel et al. [5] addressed these issues by determining all possible event types; this is not appropriate in the current simulation for two reasons. The number of different possible event types in the simulation code described here is very large since it is possible to have different types of site, first- and second-nearest-neighbour interactions and an arbitrary number of species. In addition the flexibility of adding new types of event means that it is not possible a priori to determine which events can occur, the structure of the simulation code must reflect this flexibility. The approach adopted is therefore as follows. A linked-list of all possible events is constructed and for each event a list is maintained,

as part of the event object, of all possible sites affected by this event if it were to occur. Similarly, as part of the site object, a list of all possible events that may affect this site is maintained. Only those events are used that result in a successful outcome, and a modified probability is defined as follows:

$$p'(n) = \frac{\Lambda(s, s')\mu_n}{\sum_m^{N_E} \Lambda(s, s')\mu_m}, \quad (9)$$

where $\Lambda(s, s')$ is unity if the event is allowed and zero otherwise; these probabilities are used to select an event, but the simulation time is incremented according to Eq. (3), thereby allowing for null events. A random number is generated ($0 < r \leq 1$) and used to select the next event, such that the event selected, M , is the first event to satisfy

$$\sum_n^M p'(n) \geq r. \quad (10)$$

An exhaustive search of the list of possible events is slow since this operation scales as order N_E . Instead a binary tree is used to find the next event resulting in a search for the next event scaling as $\log(N_E)$. Full details of this implementation will be given elsewhere. Having selected and implemented the selected event the list of events can be updated using the event-to-site and site-to-event pointer lists which allow only those parts of the lattice affected by the event that has just occurred to be updated. This approach results in a highly efficient code enabling many millions of Monte Carlo steps to be achieved on lattices as large as 30 000 sites in approximately 6 h of CPU time on a DEC alpha workstation.

3. Experimental

A summary of the experimental details concerning the acquisition of the ^2H NMR data is now given. The adsorbates used in this study were fully deuterated ethene and ethane (C_2D_4 and C_2D_6) and were supplied (K&G Canada) with a minimum purity of 99.5%; no further purification was used. All experimental details have been given elsewhere [8]. Accurate loadings of sorbate in the zeolite were obtained by volumetric techniques. Following loading, the sample was heated at 353 K for 4 h to ensure a homogeneous distribution of sorbate. The accuracy of the loading technique was checked by performing reproducibility tests, all of which showed excellent agreement between sample preparations.

^2H NMR spectra of each sample were recorded in the temperature range 160–370 K on a Bruker MSL 200 NMR spectrometer operating at a frequency ($\omega_0/2\pi$) of 30.72 MHz. Spin-lattice relaxation times, T_1 , and spin-spin relaxation times, T_2 , were recorded in the same temperature range, using a saturation recovery and quadrupolar spin-echo pulse sequence, respectively. The temperature was allowed to equilibrate for at least 1 h before data acquisition

commenced and was maintained stable during acquisition to 0.5 K.

4. Experimental results and analysis

4.1. Analysis of ^2H NMR data

As discussed in an earlier paper [16] estimates of the parameters describing sorbate motion are sensitive to the method chosen for the analysis of the ^2H NMR relaxation time data. In that work it was proposed that the fit parameters were much better constrained if simultaneous fitting to the temperature-dependence of both spin–spin and spin-lattice relaxation time data was performed. Hence to proceed further, analytical expressions relating sorbate motion to the temperature-dependence of the ethane and ethene T_1 and T_2 relaxation times are required. These were obtained as described below.

The dynamics of a deuterated molecule can be described in a reduced form by an auto-correlation function, $g(t)$ [17,18]. Provided the motion represented by this auto-correlation function proceeds on a time scale that is faster than the characteristic NMR time scale, τ_{NMR} , then this motion will contribute to the relaxation process. Defining the spectral density function, $j(\omega)$, as the Fourier transform of the auto-correlation function:

$$j(\omega) = 2 \int_0^{\infty} g(t) \cos \omega t \, dt, \quad (11)$$

the relaxation times T_1 and T_2 can be written as

$$\frac{1}{T_1} = k^Q (j(\omega_0) + 4j(2\omega_0)) = k^Q J_{r_1}, \quad (12)$$

and

$$\frac{1}{T_2} = k^Q \left(\frac{3}{2}j(0) + \frac{5}{2}j(\omega_0) + j(2\omega_0) \right) = k^Q J_{r_2}. \quad (13)$$

In this expression k^Q is a constant given by $(3\pi^2/4)(e^2qQ/h)^2$, where Q is the nuclear quadrupole moment and q is a principal component of the electric field gradient tensor. Considering a motion that can be described by a pure isotropic tumbling of a molecule in space (as may occur during the unrestricted translation of the molecule) then the appropriate form for the auto-correlation function is

$$g(t) = 1/5 \exp(-t/\tau_m), \quad (14)$$

where τ_m is the correlation time for this motion. In this case the spectral density function becomes

$$j(\omega) = \frac{2}{5} \frac{\tau_m}{1 + \omega^2 \tau_m^2}. \quad (15)$$

In the present analysis we apply the approach of Lipari and Szabo [19] which assumes that the motion can be

factored into a number of independent motions. The form of the correlation function including isotropic tumbling, some internal motion such as fast rotation and a librational distortion of the molecule is given by

$$g(t) = \frac{1}{5} \exp(-t/\tau_m)(S^2 + (1 - S^2) \times \exp(-t/\tau_R))(S_L^2 + (1 - S_L^2) \exp(-t/\tau_L)). \quad (16)$$

In this expression S is regarded as a free parameter, a “generalised order parameter”. For the case of isotropic rotation together with fast rotation about a preferred axis we can identify the order parameter as $S^2 = \langle d_{00}^2(\theta) \rangle$, i.e. a mean square deviation, characterised by an angle θ , of the axis of the C–D bond from its equilibrium position, and τ_R is a rotational correlation time. τ_L and S_L are the librational correlation time and order parameter, respectively.

The expressions for T_1 and T_2 used in the analysis of the ethane and ethene data presented in this work then follow:

$$\frac{1}{T_j} = \frac{3\pi^2}{4} \left(\frac{e^2qQ}{h} \right)^2 [S^2 \{S_L^2 J_{rj}(\tau_m) + (1 - S_L^2) J_{rj}(\tau_{mL})\} + (1 - S^2) \{S_L^2 J_{rj}(\tau_{mR}) + (1 - S_L^2) J_{rj}(\tau_{mRL})\}], \quad (17)$$

where $j=1,2$ and the combined correlation times are defined by

$$\frac{1}{\tau_{mL}} = \frac{1}{\tau_m} + \frac{1}{\tau_L}, \quad \frac{1}{\tau_{mR}} = \frac{1}{\tau_m} + \frac{1}{\tau_R}, \quad \frac{1}{\tau_{mRL}} = \frac{1}{\tau_m} + \frac{1}{\tau_{Rs}} + \frac{1}{\tau_L}. \quad (18)$$

The temperature dependence of the system is described by assuming each correlation time τ_i represents an activated process and can therefore be written in the form of an Arrhenius expression [17]:

$$\tau_i = \tau_{0i} \exp(E_i/RT), \quad (19)$$

where τ_{0i} is a constant and E_i is the activation energy associated with the particular motion, i . Such a description is particularly appropriate in the context of molecular motion in zeolites where models involving activated jump processes have proved successful.

4.2. Results of the ^2H NMR analysis

Loadings of approximately 2, 4 and 8 molecules per unit cell were used for both C_2D_4 and C_2D_6 . In the analysis the preferred axis of rotation was assumed to be the carbon–carbon double bond and the carbon–carbon bond (equivalent to a fast rotation of the methyl group) for C_2D_4 and C_2D_6 , respectively. The results of simultaneous fitting of the T_1 and T_2 data are given in Table 1.

In an earlier study of ethane and ethene in NaA [8], a cage-based zeolite, a good fit to the data was obtained by allowing for translational and rotational motion for both species, whereas for C_2D_6 a librational motion was also required. In silicalite the motion of these two adsorbed species is significantly modified. Firstly, a librational mode

Table 1
 ^2H NMR relaxometry results for C_2D_4 and C_2D_6 sorbed in silicalite (loadings are given as molecules per unit cell)

	Loading	E_m (kJ/mol) ± 0.5	τ_{m0} (s) $\pm 5\%$	E_R (kJ/mol) ± 5	τ_{R0} (s) $\pm 20\%$	$S_L \pm 0.01$
C_2D_4	2.0	14.3	2.5×10^{-9}	30.0	1.1×10^{-14}	0.49
C_2D_4	4.0	11.9	4.0×10^{-9}	26.3	4.0×10^{-14}	0.60
C_2D_4	8.0	11.8	4.3×10^{-9}	20.6	4.3×10^{-15}	0.84
C_2D_6	2.6	12.5	6.0×10^{-8}	30.0	6.2×10^{-17}	0.17
C_2D_6	4.0	13.3	2.0×10^{-8}	30.0	1.8×10^{-17}	0.20
C_2D_6	8.0	9.4	2.8×10^{-8}	30.0	1.9×10^{-17}	0.10

is necessary for a good fit for both the C_2D_4 and C_2D_6 data, consistent with both species having restricted motion within the silicalite framework; however, the librational order parameter is much smaller for C_2D_6 consistent with the relatively large size of the methyl group. Also apparent is the very long time scale for the isotropic reorientation of the molecule. This is consistent with isotropic motion not being possible in the vicinity of an adsorption site, i.e. the molecule is not free to rotate in an arbitrary fashion even when not bound closely to an adsorption site. This is consistent with both our MD simulations and the need for large librational terms in the relaxometry analysis. The time scale for rotation about a preferred axis is however considerably shorter suggesting that this process occurs relatively easily within the silicalite channels. A simple interpretation of these data is that both ethane and ethene can undergo rotation about this preferred axis when not directly adsorbed, as in jumps between adjacent adsorption sites. The picture is of a molecule that retains the axis defined by the C–C bond (also the axis of preferred rotation) approximately aligned with the direction of the zeolite channel during translational motion. This interpretation implies that the rotational time scales and activation energies obtained from the ^2H NMR relaxometry analysis should be taken to most closely describe the desorption of the sorbates from sites within the silicalite framework, and therefore it is these values that should be associated with the corresponding time scale and activation energies of the jump event within the MCLD simulation. This interpretation is also supported by the large activation energy to the rotational motion which is more characteristic of a desorption event than an internal molecular motion; the molecule must first desorb from a site before rotation is possible. The time scale determined from the NMR data is a dynamical correlation time for the motion and is not directly related to the attempted jump-rate from a site, therefore interpreting the pre-exponential factors in terms of a jump frequency is not appropriate. The activation energy to the rotational motion, E_R , for ethene indicates a decrease in the activation energy for site-to-site jumps with increasing sorbate loading. This observation is consistent with a repulsive interaction energy between adsorbed ethene molecules; no such decrease is observed from the ethane analysis in the case of single-component adsorption.

5. MCLD simulation of adsorption isotherms and comparison with experiment

The approach to modelling the adsorption isotherms consist of three steps. Firstly, the results of the ^2H NMR analysis are used to constrain as far as possible the input parameters to the MCLD simulation. Secondly, acceptable ranges for model parameters not constrained by the NMR analysis are determined by fitting the single-component isotherms. Finally, the binary-component isotherms are determined using the constrained data.

As shown in Fig. 1, there are three distinct types of site present characterised by different activation energies to desorption. Further, the 28 distinct sites within the unit cell cannot be simultaneously occupied. This effect is modelled by introducing a repulsive interaction energy for molecules on adjacent sites. In the equilibrium configuration of molecules within the zeolite, as probed by the ^2H NMR experiment, we do not expect adjacent sites to be occupied. The ^2H NMR results will therefore not provide a direct measure of this interaction energy and we must therefore treat this parameter as a variable. Our MD simulations suggest that the rate of desorption from each of the 0, I and II sites are similar at 300 K, and that the activation energies to desorption from these sites satisfy $E_{II} \approx E_I + 3 \text{ kJ/mol} \approx E_0 + 6 \text{ kJ/mol}$. Therefore at 323 and 348 K desorption from type 0 sites will be fastest and hence molecules at these sites are likely to dominate the observed NMR relaxation process. We therefore associate the activation energy for site desorption determined from the NMR data at low loadings, E_R , with the type 0 sites ($E_{0i} = E_R$, $i=0,1$). The results are somewhat insensitive to this assignment and agreement with the single-component isotherms can be achieved by assigning $E_{1i} = E_R$ with changes to other parameters. For the remainder of this paper we will consider only results with the assignment $E_{0i} = E_R$. For ethane–ethane (species 0) the constancy of the rotational activation energy with loading is taken as evidence for no additional molecule–molecule interaction beyond nearest-neighbour. For ethene–ethene (species 1) an additional second-nearest-neighbour repulsive interaction is included, constrained by the ^2H NMR analysis reported in Table 1, giving $E_{00}^{(2)} = 0$, $E_{11}^{(2)} = 3 \text{ kJ/mol}$. The activation energy to desorption on adjacent sites was found from an investigation of parameter space,

and values of $E_{00}^{(1)} = 4$, $E_{11}^{(1)} = 8$ kJ/mol for this parameter were found to give best agreement with experimental data for the single-component isotherms. All simulations reported here were performed on a lattice consisting of $8 \times 8 \times 8$ unit cells.

The pre-exponential factor for the residence time for each specie can also, in principle, be determined from the NMR data. However, the experimental result is not well constrained due to the strong interdependence with the order parameters for the respective librational motions and therefore the NMR analysis gives only an order of magnitude estimate for this parameter. Furthermore when Eqs. (5) and (8), describing the two principle event types, are cast in dimensionless form it is necessary to introduce a characteristic time scale, t_0 . It is convenient to select this time scale so as to make the rates of order unity and for computational convenience we select the characteristic time scale to be that of the residence time of species 0 at site 0 at $T=300$ K:

$$t_0 = \tau_{00} \exp(E_{s0}/300 R). \quad (20)$$

With this choice of characteristic time scale and after re-writing all jump rates in dimensionless form it is clear that all site-to-site jump rates are relative to the time scale t_0 and the group $(t_0 \alpha_i)$ enters the expression for the attempted insertion rate (Eq. (8)). Since the relative jump rate is fixed by the NMR results, and α_i must already be regarded as an adjustable parameter it is appropriate to regard $(t_0 \alpha_i)$ as a single adjustable parameter to be determined from fitting to the experimental data.

5.1. Single-component adsorption isotherms

As discussed above, for the prediction of single-component isotherms, there exist two free parameters for each species ($t_0 \alpha_i, E_{ii}^{(1)}$); all other model parameters are constrained to within the experimental error of the ^2H NMR data. Simulation of the experimentally determined isotherms is achieved by generating a range of models that are consistent with the constraints of the ^2H NMR analysis and the observed isotherms. The results are shown in Fig. 2. Excellent agreement between predicted and experimental

Table 2

Simulation parameters used in the modelling of single- and binary-component adsorption isotherms (all energies are given in units of kJ/mol)

Parameter	C_2H_6	C_2H_4
$t_0 \alpha_i$ (10^{-9} s)	6.7	4.8
E_{0i}	30.5	26.5
E_{1i}	33.5	29.5
E_{11i}	36.5	32.5
$E_{ij}^{(1)}$	4.0	8.0
$E_{ij}^{(1)}$	8.0	8.0
$E_{ij}^{(2)}$	0.0	3.0
$E_{ij}^{(2)}$	3.0	3.0

isotherms is achieved over the full range of pressure investigated experimentally. The model parameters consistent with the results of the ^2H NMR analysis and that give best agreement with the measured isotherms are given in Table 2. The results for the single-component isotherms are rather insensitive to the values chosen for the molecule–molecule interaction energies on both first- and second-nearest-neighbour sites; these parameters are however tightly constrained by the binary-component isotherms discussed in the next section. The overall variation of the isotherm with temperature is strongly dependent on the activation energies for site-to-site jumps. The latter are constrained by the NMR relaxation data to within ± 1 kJ/mol for good agreement between the predictions of the model and experimental data.

Having determined those parameters not fully constrained by the ^2H NMR data, the model becomes predictive in that isotherms at arbitrary temperature can be simulated and compared to experimental data. This is done for the single-component isotherms in Fig. 2 where the set of model parameters determined from NMR data and fitting to the isotherm data at 323 K are used to predict the adsorption isotherms for both ethane and ethene at 348 K. The agreement between adsorption data in the range 323 and 348 K is well modelled using the MCLD approach including a minimal number of possible events – site desorption followed by re-adsorption to an adjacent site. Other types of event, such as for example surface diffusion,

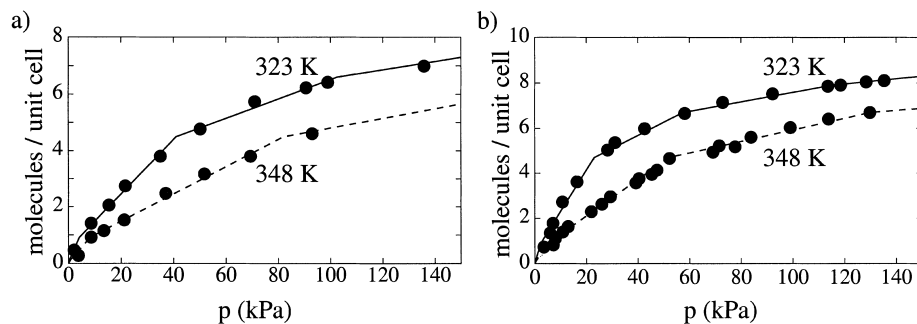


Fig. 2. Single-component adsorption isotherms for silicalite. The MCLD simulation results (lines) are compared to experimental data (solid points) [11] for (a) ethene and (b) ethane.

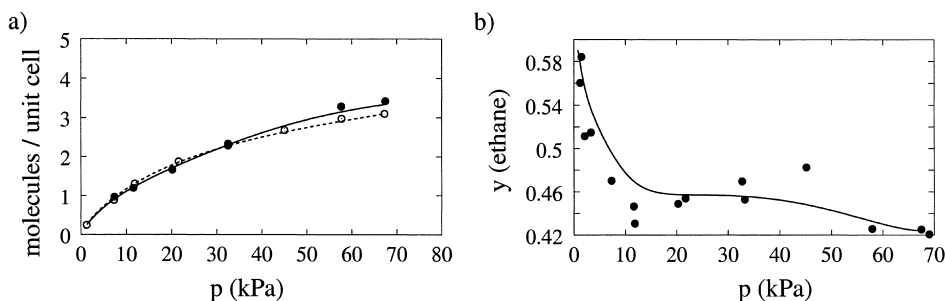


Fig. 3. Binary-component adsorption isotherms for silicalite. (a) The MCLD simulation results (lines) are compared to experimental data (points) [11] for ethane (—, ●) and ethene (- - -, ○). (b) Gas-phase mole fraction of ethane in equilibrium with a 50:50 binary mixture adsorbed within the zeolite; model prediction (—), experimental data (●).

are not included in the model and are not required to explain the adsorption data presented. However, the existence of such processes, when they occur on time scales faster than those associated with the events considered in the present analysis, may be important in explaining other experimental measurements. In the following section the predictive power of the model is further demonstrated by simulating binary-component isotherms using parameters obtained from modelling the single-component data.

5.2. Binary-component isotherms

The experimental results for the binary-component adsorption studies are presented in two ways:

1. Adsorbed phase composition as a function of total external gas pressure for an initially 50:50 gas-phase composition.
2. Gas-phase mole fraction of ethane as a function of total external gas pressure for an approximately 50:50 composition within the zeolite.

Three additional parameters are introduced in modelling the binary-component data, namely the ethane–ethene interaction energy on first- and second-nearest-neighbour sites, and the ratio of residence times for ethene to ethane on type 0 sites. The ethane–ethane and ethene–ethene first-nearest-neighbour interactions were taken to be 4 and 8 kJ/mol, respectively, as determined from the single-component analysis. Preliminary ^2H NMR data for ethane–ethene mixtures in silicalite show a decrease in the rotational activation energy with increasing ethene loading at constant ethane loading and vice versa. The magnitude of this effect with increasing loading is similar to that seen for the ethene–ethene interaction. The first-nearest-neighbour ethane–ethene interaction was therefore taken to be fixed at 8 kJ/mol, and further, we consider only those models in which the ethane–ethene second-nearest-neighbour interaction has the same value as that for ethene–ethene.

The comparison of the experimentally determined isotherm data with the MCLD predictions is shown in Fig. 3; agreement is excellent. Such good agreement is particularly

noteworthy given that the non-ideality of the binary-component behaviour has been predicted whilst all input data to the MCLD simulation (Table 2) have been constrained by independent experimental data.

5.3. Discussion

In the MCLD model, adsorption is modelled explicitly by following the kinetics of the adsorbed and gas-phase species. Equilibrium corresponds to the existence of a detailed balance between all possible events both within the MCLD lattice representing the zeolite–sorbate system and between the lattice and the gas phase. The results obtained permit insight into the rate of site-desorption events of the adsorbed species. At low loadings molecule–molecule interactions are minimal. In this case the adsorption is dominated by the intrinsic rate of site-desorption events of each adsorbed species within the zeolite; the species with the fastest rate of site desorption establishes a dynamic equilibrium with the gas phase such that fewer molecules are adsorbed. At low loading, ethane has a higher site-desorption rate than ethene and therefore near equal loadings of each species are achieved with an ethane-rich external atmosphere. As the loading of both species increases the strong ethene–ethene and ethene–ethane repulsions become increasingly important resulting in an increase in the rate of site-desorption of ethene. Eventually at high loadings ethene achieves a faster rate of site desorption than ethane and the dynamic equilibrium with the gas phase is satisfied by an ethene-rich external gas phase.

6. Conclusions

A flexible and efficient MCLD simulation code has been developed to enable a range of problems to be investigated involving bulk or collective motions of molecules adsorbed within a pore space. The modelling strategy aims to produce a realistic representation of the structure of the adsorbent by associating lattice sites with adsorption sites, and connectivities of the MCLD lattice chosen to reproduce the topology and geometry of the zeolite of interest. Experi-

mental data, and/or MD and GCMC simulations, can then be used to constrain many aspects of the simulation lattice. In this work, the results of an analysis of the temperature-dependence of ^2H NMR relaxation-time behaviour of the sorbed species in terms of their motional characteristics are used to constrain the input parameters to the MCLD model.

We have illustrated the application of this method for the case of single- and binary-component adsorption of ethane and ethene in silicalite. ^2H NMR relaxometry data constrain all but two parameters of the model for each species in the case of single-component adsorption. The remaining two parameters are then constrained by the fit of the MCLD results to the experimentally determined isotherm data. Having assigned values to these two parameters the MCLD simulation is able to predict the temperature-dependence of the single-component isotherms. The same parameters are then used in the MCLD simulations of the binary-component isotherms. In the cases of both single- and binary-component adsorption, excellent agreement between simulated and experimental isotherms is obtained and the results have been interpreted in terms of the relative rates of site desorption of adsorbed species within the zeolite framework.

Acknowledgements

LFG wishes to thank EPSRC for the award of the NMR spectrometer. M. Hargreaves thanks BBSRC and BNFL Research & Technology for financial support.

References

- [1] J. Kärger, D.M. Ruthven, *Diffusion in Zeolites*, Wiley, New York, 1992.
- [2] E. Cohen de Lara, R. Kahn, A.M. Goulay, *J. Chem. Phys.* 90 (1989) 7482–7491.
- [3] R.L. June, A.T. Bell, D.N. Theodorou, *J. Phys. Chem.* 96 (1992) 1051–1060.
- [4] E. Hernández, C.R.A. Catlow, *Proc. R. Soc. London A* 448 (1995) 143–160.
- [5] P.R. van Tassel, S.A. Somers, H.T. Davis, A.V. McCormick, *Chem. Eng. Sci.* 49 (1994) 2979–2989.
- [6] D.N. Theodorou, J. Wei, *J. Catal.* 83 (1983) 205–224.
- [7] P.H. Nelson, A.B. Kaiser, D.M. Bibby, *J. Catal.* 127 (1991) 101–112.
- [8] L.F. Gladden, J.A. Sousa-Gonçalves, P. Alexander, *J. Phys. Chem. B.* 101 (1997) 10121–10127.
- [9] M.-O. Coppens, A.T. Bell, A.K. Chakraborty, *Chem. Eng. Sci.* 53 (1998) 2053–2061.
- [10] D. Keffer, A.V. McCormick, H.E. Davis, *J. Phys. Chem.* 100 (1996) 967–973.
- [11] M. Hargreaves, Ph.D. Thesis, University of Cambridge, Cambridge, 1999.
- [12] C. Saravanan, F. Jousse, S.M. Auerbach, *Phys. Rev. Lett.* 80 (1998) 5754–5757.
- [13] D.M. Ford, E.D. Glandt, *J. Membr. Sci.* 107 (1995) 47–57.
- [14] M. Hargreaves, A.S. Mcleod, L.F. Gladden, *Proceedings of Fundamentals of Adsorption, FOA6*, May 1998.
- [15] J.K. Ousterhout, *Tcl and the Tk Toolkit*, Addison-Wesley, New York, 1994.
- [16] J.A. Sousa-Gonçalves, R.L. Portsmouth, P. Alexander, L.F. Gladden, *J. Phys. Chem.* 99 (1995) 3317–3325.
- [17] H. Pfeifer, in: P. Diehl, E. Fluck, R. Kosfeld (Eds.), *NMR Basic Principles and Progress*, vol. 7, Springer, New York, 1972, pp. 55.
- [18] H.W. Speiss, in: P. Diehl, E. Fluck, R. Kosfeld (Eds.), *NMR Basic Principles and Progress*, vol. 15, Springer, New York, 1978, pp. 54.
- [19] G. Lipari, A. Szabo, *J. Am. Chem. Soc.* 104 (1982) 4546–4559.